Role of hydrophobic interactions in yeast phosphoglycerate kinase stability

ARTICLE *in* PROTEINS STRUCTURE FUNCTION AND BIOINFORMATICS · MARCH 2000

Impact Factor: 2.63 · DOI: 10.1002/(SICI)1097-0134(20000201)38:2<226::AID-PROT10>3.0.CO;2-H · Source: PubMed

5 AUTHORS, INCLUDING:

Dominique Durand
Université Paris-Sud 11
124 PUBLICATIONS **2,608** CITATIONS
SEE PROFILE

Patrice Vachette
French National Centre for Scientific Resea…
101 PUBLICATIONS **2,274** CITATIONS
SEE PROFILE

PROTEINS: Structure, Function, and Genetics 38:226–238 (2000)

Role of Hydrophobic Interactions in Yeast Phosphoglycerate Kinase Stability

Veronique Receveur,[1] Pascal Garcia,[1] Dominique Durand,[2] Patrice Vachette,[2] and Michel Desmadril[1]*
[1]*Laboratoire de Modélisation et Ingénierie des Protéines, Université de Paris-Sud Orsay Cedex, France*
[2]*Laboratoire pour l'Utilisation du Rayonnement Electromagnétique (CNRS/CEA/MENRT) Université de Paris-Sud, Orsay Cedex, France*

ABSTRACT **Cold denaturation of yeast phosphoglycerate kinase (yPGK) was investigated by a combination of far UV circular dichroism (CD), steady-state and time-resolved fluorescence, and small angle X-ray scattering. It was shown that cold denaturation of yPGK cannot be accounted for by a simple two-state process and that an intermediate state can be stabilized under mild denaturing conditions. Comparison between far UV CD and fluorescence shows that in this state the protein displays a fluorescence signal corresponding mainly to exposed tryptophans, whereas its CD signal is only partially modified. Comparison with spectroscopic data obtained from a mutant missing the last 12 amino-acids (yPGK Δ404) suggests that lowering the temperature mainly results in a destabilization of hydrophobic interactions between the two domains. Small angle X-ray scattering measurements give further information about this stabilized intermediate. At 4°C and in the presence of 0.45 M Gdn-HCl, the main species corresponds to a protein as compact as native yPGK, whereas a significant proportion of ellipticity has been lost. Although various techniques have shown the existence of residual structures in denatured proteins, this is one example of a compact denatured state devoid of its main content in alpha helices. Proteins 2000;38: 226–238.** © 2000 Wiley-Liss, Inc.

Key words: phosphoglycerate kinase; cold denaturation; hydrophobic interactions; SAXS

INTRODUCTION

Our understanding of the energetics of protein folding and structure requires a complete description of thermodynamic stability. This need has led to numerous thermodynamic studies of protein folding. Although heat denaturation has been the main approach, many studies have shown that proteins also undergo a reversible unfolding when the temperature is lowered.[1,2] Cold denaturation was first predicted by Brandts[3] in 1964 and then by Privalov[4] in 1979. However, its direct characterization was only firmly established in 1986 by Privalov with his work on myoglobin,[5] for which cold destabilization was observed at a temperature close to 0°C. Actually, cold denaturation should occur for many proteins in solution but at subzero temperature and, therefore, cannot be observed. However, one can achieve cold denaturation at experimentally accessible temperatures with the help of a partial destabilization by pH, pressure, addition of chaotropic solutes,[4] or changing salt concentration in the case of halophilic proteins.[6] Thus, various studies have dealt with protein unfolding induced by decreasing temperature.[2] Although cold denaturation of proteins is now a well-recognized phenomenon, little is known about the structure of cold-denatured states of proteins. Only for a few proteins was the cold denatured state shown to be equivalent to the heat denatured one.[7] In most cases, almost nothing is known about the compactness and the flexibility of cold-denatured proteins, although differences have been observed in the denaturation process.[8–10] Such knowledge could provide crucial information about the role of hydrophobic interactions on the stabilization of the protein structure.

Previous studies performed in our laboratory[11–13] have led to insights about the relative contribution of various types of interaction in the stability of a model protein, i.e., yeast phosphoglycerate kinase (yPGK). yPGK (EC 2.7.2.3.) is a glycolysis enzyme catalyzing the transfer to ADP of the phosphoryl group of 1,3 diphosphoglycerate to produce ATP. This monomeric protein consists of 415 amino acids and is folded into two globular domains of equal size linked by a hinge. yPGK contains two tryptophans, both located in the C-terminal domain. yPGK is one of the first proteins in which cold denaturation has been revealed. Griko and co-workers first performed CD, fluorescence and DSC experiments and showed that yPGK was denatured at low temperature when additionally destabilized by 0.7 M Gdn-HCl.[14] Freire and co-workers confirmed these results

Abbreviations: CD, circular dichroism; DLS, dynamic light scattering; EDTA, ethylene diamine tetraacetate; Gdn-HCl, guanidine hydrochloride; Rg, Radius of gyration; SAXS, small angle X-ray scattering; Tris, Tris(hydroxymethyl) aminomethane; yPGK, yeast phosphoglycerate kinase (E.C. 2.7.2.3); yPGK Δ404, yeast phosphoglycerate kinase mutant devoid of the last 12 amino acids.

Grant sponsor: Centre National de la Recherche Scientifique; Grant sponsor: Ministère de l'Enseignement Supérieur et de la Recherche.

Dr. Receveur's present address is AFMB-CNRS 31 Chemin Joseph Aiguier, 13402 Marseille, Cedex 20 France.

Dr. Garcia's present address is Instituto de Estructura de la Materia, CSIC, Serrano 119, 28006, Madrid, Spain.

*Correspondence to: Michel Desmadril, Laboratoire de Modélisation et Ingénierie des Protéines, Bât 430, Université de Paris-Sud Orsay Cedex, France.

Received 3 June 1999; Accepted 14 September 1999

and interpreted their findings in the same way: the N-terminal domain was less stable than the C-terminal domain at low temperature.[15] Damaschun and co-workers completed these studies and added to the previous techniques DLS and SAXS to investigate this process.[16–19] They showed that the previous interpretation was wrong, as the N-terminal domain is indeed less cold sensitive than the C-terminal domain. Moreover, they described cold-denatured yPGK as an expanded chain close to a random coil. Thus, the cold denaturation of yPGK is a process that may involve more than two species in equilibrium. However, all these studies were performed under specific destabilizing conditions: in the presence of 0.7 M of Gdn-HCl. Different conditions may then modify the distribution of these species in solution and the characteristics of the observed cold-denatured state may therefore be completely different.

Here, we report the results of a detailed investigation of the cold denaturation of yPGK carried out for a wide range of denaturant concentrations, by using circular dichroism, steady-state and time-resolved fluorescence and small angle X-ray scattering. To understand better the role of the interactions between the two domains, we performed the same experiments on both the wild-type protein and a mutant, yPGK Δ404, devoid of the last 12 amino-acids, which form the helix XIV locking the C-domain onto the N-domain. Indeed this mutant was shown to display the sum of the properties of the two isolated domains.[13,20] The large uncoupling of the domains has been ascribed to the loss of key hydrophobic interactions. Thus, a direct comparison between the cold denaturation of wild-type yPGK and yPGK Δ404 could help and confirm our hypothesis about the role of hydrophobic interactions between the domains.

MATERIALS AND METHODS

Wild-type yPGK and yPGK Δ404 were prepared as described previously.[13] All measurements were performed in a 20 mM Tris-HCl buffer, pH 7.5, containing 0.5 mM EDTA and 1 mM 2-mercaptoethanol.

Equilibrium Studies as a Function of Gdn-HCl Concentration

The unfolding experiments were carried out with a 2 μM protein concentration. The circular dichroism and fluorescence measurements were performed after 12 hours of incubation at 20°C or 4°C in various Gdn-HCl concentrations. Ultrapure Gdn-HCl was obtained from Pierce; the denaturant concentrations were checked by refractometry, by using the relationship provided by Nozaki.[21] The transition curves were constructed by plotting either the variation in ellipticity at 220 nm or the position of maximum fluorescence emission as a function of denaturant concentration.

Thermodynamic analysis was performed by using the model of linear dependency of ΔG_x on denaturant concentration x according to Pace:[22]

$$\Delta G_x = \Delta G_0 - m\,x \qquad (1)$$

where ΔG_0 being the standard variation of free energy in the absence of denaturant and m a constant proportional to the increase in the degree of exposure of protein to solvent on denaturation. The transitions curves were fitted to an equation derived from Equation 1, taking into account both the baselines and the transition region:

$$y_x = y_n + s_n x + \left\{ \frac{e^{\left[\frac{\Delta G_0 - mx}{RT}\right]}}{1 + e^{\left[\frac{\Delta G_0 - mx}{RT}\right]}} \right\} [A + (s_d - s_n)x] \qquad (2)$$

where y_x is the experimental signal in the presence of x molar Gdn-HCl, y_n the signal of the native form, s_n and s_d are the solvent effects on the native and denatured protein signal, respectively, and A is the amplitude of the transition. Such a function, representative of a two-state process:

$$N \overset{\Delta G}{\Leftrightarrow} D$$

gives a sigmoid curve, the mid-point transition Cm corresponding to the denaturant concentration for which $\Delta G_{cm} = 0$. For asymmetrical transition curves, the transition region was described by a linear combination of two single-transition curves:

$$y_x = y_n + s_n x + \left[\frac{\alpha\, e^{\left[\frac{(\Delta G_{0,1} - m_1 x}{RT}\right]}}{1 + e^{\left[\frac{(\Delta G_{0,1} - m_1 x)}{RT}\right]}} + \frac{(1-\alpha)\, e^{\left[\frac{(\Delta G_{0,2} - m_2 x)}{RT}\right]}}{1 + e^{\left[\frac{(\Delta G_{0,2} - m_x x)}{RT}\right]}} \right] [A + (s_d - s_n)x] \qquad (3)$$

with distinct parameters $\Delta G_{0,i}$and m_i, α corresponding to the relative amplitude of the first transition. Such an equation corresponds to a three-state model of the denaturation process:

$$N \overset{\Delta G1}{\Leftrightarrow} X \overset{\Delta G2}{\Leftrightarrow} D$$

Experimental data were fitted according to Equation 2 or 3 by using a simplex procedure based on the Nelder and Mead algorithm.[23]

Melting Curves of yPGK

Melting curves of yPGK were monitored by using circular dichroism and fluorescence signal of a 2 μM protein solution. After 12 hours of incubation at 4°C, the solution was heated at 0.5 K/min. CD signal was continuously recorded at 220 nm by using a computer, whereas for fluorescence measurements, emission spectra were recorded every 2°C step between 330 and 360 nm. It was verified that there was no significant change in the fluorescence spectra during time recording.

Time-Resolved Fluorescence

Fluorescence decays were measured at 350 nm by the single photoelectron counting method[24] on protein samples prepared as for equilibrium studies with a final protein concentration of 30μM. The experimental set-up, recording conditions and time-resolved analysis were identical to those described in previous studies.[25]

Small Angle X-Ray Scattering

Scattering patterns were recorded on the D24 small-angle scattering instrument D24 installed on a bending magnet of the storage ring LURE- DCI (Orsay, France) by using a wavelength λ = 1.488 Å. The instrument,[26] the data-acquisition system,[27] and the evacuated sample cell[28] have already been described. The distance from the sample to the linear position-sensitive detector was about 2,070 mm, giving access to scattering vectors q ranging from 0.01 up to 0.17 $Å^{-1}$. The scattering vector is defined as $q = 4\pi\lambda^{-1}\sin\theta$ where 2θ is the scattering angle. The temperature of the sample was controlled by circulating temperature-controlled water. To avoid radiation-induced protein damage, dithiothreitol was added to all solutions to a final concentration of 1 mM. Moreover, the protein solution was continuously circulated through the quartz capillary. Exposure to the X-ray beam, thus, was kept shorter than 15 minutes. A preliminary 25-minute-long exposure without circulation did not show any radiation damage. Eight successive frames of 200 seconds each were recorded for each curve and subsequently averaged after visual inspection. The protein concentration was 5 mg/ml. The scattering from buffer solutions at the same Gdn-HCl concentration was measured and subtracted from the corresponding protein solution pattern after proper normalisation.

Scattering Data Analysis

The value of the radius of gyration Rg of the compact protein is derived from the Guinier approximation:

$$I(q) \cong I(0)\exp\left(-\frac{R_g^2 q^2}{3}\right) \quad (4)$$

where I(q) is the scattered intensity. It was shown[29] that for a spherical particle this approximation is valid out to $qR_g \cong 1.3$ $Å^{-1}$.

The radius of gyration of strongly denatured yPGK was determined by using the Debye function[30] as described previously:[31]

$$P(x) = \frac{I(q)}{I(0)} = \frac{2}{x^2}(x - 1 + e^{-x}) \quad (5)$$

where $x = (qR_g)^2$. The scattering profile of an expanded chain is in fact better described by this function.[31] The fitting range extended out to $qR_g \leq 3$.

The radius of gyration thus obtained is an apparent Rg corresponding to a 5 mg/ml solution. The effect of protein concentration has been discussed previously[31] and shown to be practically negligible for essentially globular objects, although significant for fully denatured protein. Because we are concerned here primarily with compact states of the protein, extrapolation of Rg values to zero protein concentration was not deemed necessary. A final word of caution is warranted about the meaning of the apparent radius of gyration derived from the scattering pattern of a mixture of conformations. If the values are not very different, they cannot be resolved and the square of the apparent value Rg_{app} yielded by the data represents a mean of the Rg^2 of the different states weighted by their respective concentration within the solution:

$$Rg_{app}^2 = \sum_i f_i Rg_i^2. \quad (6)$$

Scattering Pattern Calculations From Atomic Coordinates

The scattering from the crystallographic structure was calculated by using the program CRYSOL,[32] which takes the scattering from the solvation shell into account and fits the given experimental scattering curve by using two free parameters, the excluded volume of the particle and the contrast of the hydration layer $\delta\rho_b = \rho_b - \rho_s$, (here, ρ_s and ρ_b denote the scattering length densities of the bulk and bound solvent, respectively). The atomic coordinates were those of the yPGK structure determined by Watson and co-workers.[33] The open structures used to model the mutant yPGK Δ404 were produced by using the version 5.5 of the Turbo-Frodo program[34] running on an Indigo-2 SGI workstation. The C-terminal domain was rotated by several tens of degrees with respect to the N-terminal domain around one or two axes intercepting at the threonine 202-Cα atom located at the C-terminal end of the linker connecting the two domains.

RESULTS

Gdn-HCl Denaturation at Low Temperature

yPGK is destabilized by lowering temperature[9,16,18,19] and such phenomenon can be evidenced by performing Gdn-HCl denaturation at various temperatures. By lowering temperature from 22°C to 4°C, a clear shift in the transition midpoint (Cm) value can be observed for Gdn-HCl induced transitions monitored either by ellipticity at 220 nm or by fluorescence (Figs. 1 and 2).

When monitoring the transition by ellipticity at 220 nm, the curve obtained with wild-type yPGK is fully symmetrical at both temperatures (Fig. 1A). This indicates that, to a first approximation, the phenomenon can be analyzed according to a two-state process. With such a hypothesis and by using Equation 2 in the Materials and Methods section, thermodynamic analysis of these transitions indicates a decrease of ΔG_0 of about 3 kcal/mol, from 7.8 kcal/mol at 22°C to 4.9 kcal/mol at 4°C . This decrease in ΔG_0 corresponds to a shift in the Cm value from 0.8 to 0.5M Gdn-HCl, without any change in the cooperativity of the process (Table I).

When denaturation is monitored by a shift in the fluorescence emission maximum (Fig. 1B), the transition curves are no longer symmetrical but display two clear phases, the second one being related to residual structures.[11,25] As for CD measurements, the transition obtained at 4°C is shifted

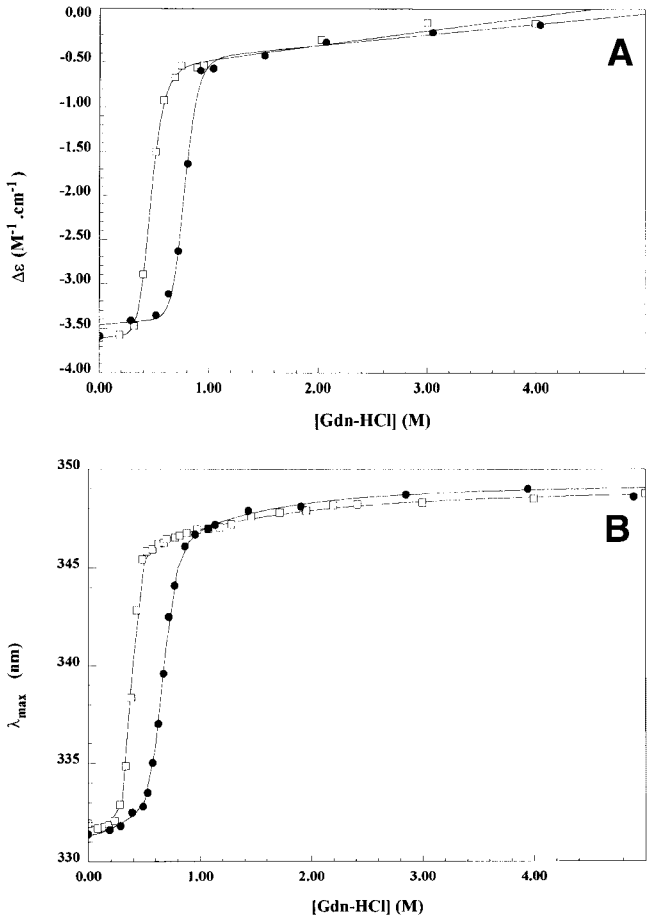

Fig. 1. Transition curve of wild-type yPGK monitored by variation of ellipticity at 220 nm (**A**) and by the shift in maximum fluorescence emission wavelength (**B**) either at 4°C (squares) or 22°C (circles).

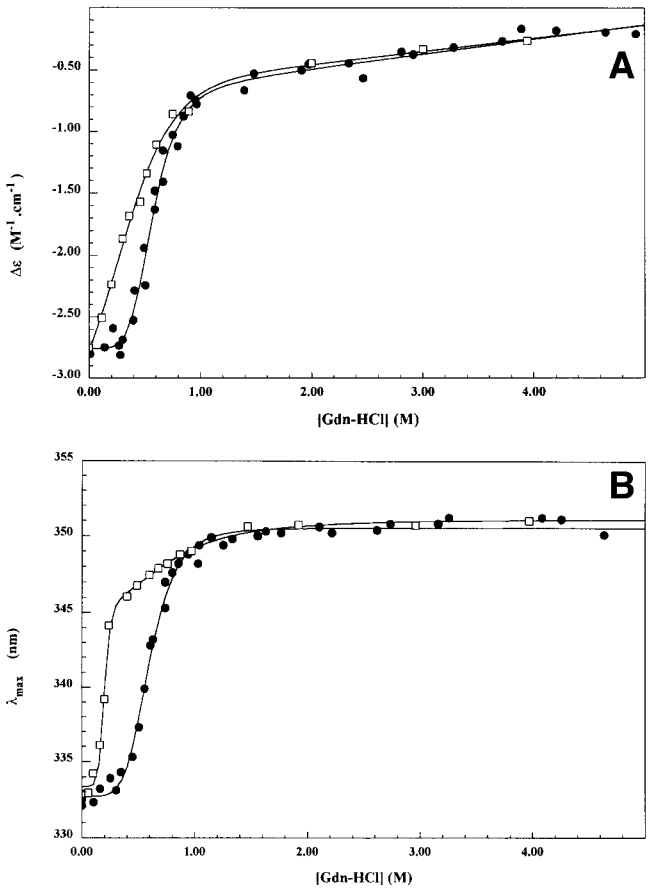

Fig. 2. Transition curve of yPGK Δ404 monitored by variation of ellipticity at 220 nm (**A**) and by the shift in maximum fluorescence emission wavelength (**B**) either at 4°C (squares) or 22°C (circles).

toward lower concentration values. This transition displays an asymmetry as observed at 22°C.

Transition curves of yPGK Δ404 were also recorded at 22°C and 4°C (Fig. 2). At 22°C, transition curves obtained by monitoring both ellipticity and fluorescence were found to be symmetrical, the Cm values being equal to 0.54 M and 0.59 M, respectively. The corresponding ΔG_0 values are comparable, equal to 2.7 kcal/mol and 2.9 kcal/mol, respectively. Transition curves obtained at 4°C indicate a destabilization of the protein and display different features from that obtained at 20°C. The transition observed by CD measurements is shifted toward lower denaturant concentration and displays a lower cooperativity at 4°C than at 22°C (Fig. 2A). The transition observed by fluorescence measurements becomes asymmetrical (Fig. 2B), displaying two well-resolved phases, the first one with a Cm of 0.2 M Gdn-HCl and the second one with a Cm of 1.15 M GdnHCl (Table I).

Cold Denaturation of yPGK in the Presence of Gdn-HCl

Melting curves were monitored by variation of ellipticity at 220 nm and shift in the maximum wavelength of fluorescence intensity at various denaturant concentrations, for both wild-type yPGK and yPGK Δ404. Because it has been checked that cold denaturation is a fully reversible process, melting curves are also refolding curves; therefore, the refolding process was monitored to reach the equilibrium state more quickly (Figs. 3 and 4).

As expected from data reported in Figures 1 and 2, the temperature effect is only observed for a particular range of denaturant concentrations, the amplitude of the melting transition obtained by both signals being directly related to this concentration. Moreover, for the highest denaturant concentrations used, the onset of protein denaturation can already be detected at room temperature.

The comparison between melting curves monitored by CD (Fig. 3A) and fluorescence (Fig. 3B) shows that the cold denaturation of wild-type yPGK is not a simple two-state process. Although melting curves monitored by fluorescence are nearly symmetrical, those obtained by CD display a clear asymmetry. For a given denaturant concentration, the cold effect is stronger on fluorescence than on the CD signal: at 0.45 M Gdn-HCl, there is 80% of the native ellipticity, whereas there is only 15% of the native fluorescence signal (Fig. 3A,B). This difference is also observed for yPGK Δ404 (Fig. 4). In fact, cold denaturation

TABLE I. Thermodynamic Parameters of the Transition Curves Reported in Figures 1 and 2[†]

	Temperature (°C)	ΔG_1 (kcal/mol)	Cm_1 (M)	M_1 (kcal · mol^{-1}M^{-1})	ΔG_2 (kcal/mol)	Cm_2 (M)	m_2 (kcal · mol^{-1}M^{-1})
WT							
CD	22	7.8 ± 0.3	0.80 ± 0.04	9.8 ± 0.2			
	4	4.9 ± 0.4	0.50 ± 0.05	9.8 ± 0.2			
Fluo	22	8.1 ± 0.3	0.75 ± 0.05	11.0 ± 0.2	1.4 ± 0.5	1.1 ± 0.3	1.5 ± 0.5
	4	6.0 ± 0.2	0.38 ± 0.06	15.0 ± 0.2	1.5 ± 0.5	1 ± 0.2	1.5 ± 0.5
Δ404							
CD	22	2.7 ± 0.3	0.54 ± 0.04	5.0 ± 0.2			
	4	1.1 ± 0.4	0.35 ± 0.05	3.0 ± 0.2			
Fluo	22	2.9 ± 0.3	0.59 ± 0.05	4.9 ± 0.2			
	4	5.1 ± 0.6	0.2 ± 0.08	25 ± 2	1.5 ± 0.5	1.1 ± 0.2	1.5 ± 0.5

[†]Confidence intervals correspond to a probability of 0.95. WT, wild type; CD, circular dichroism; Fluo, fluorescence.

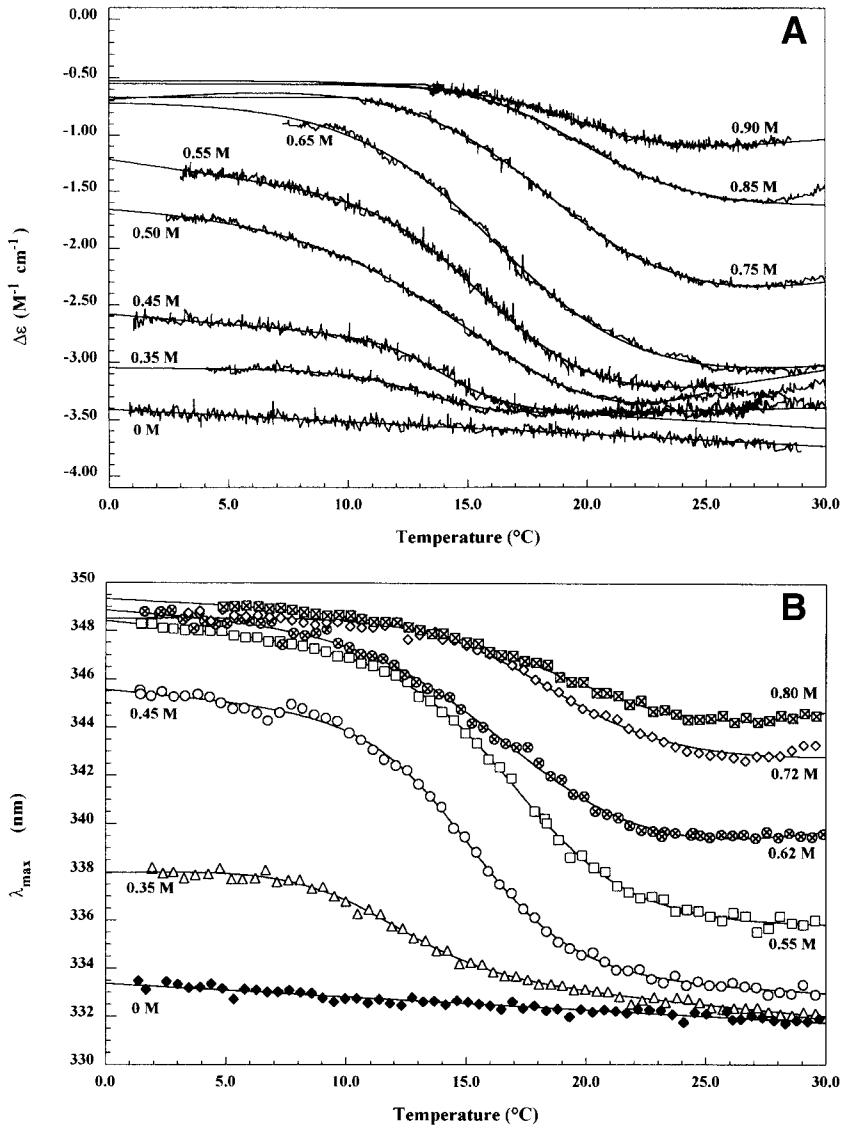

Fig. 3. Melting curves of wild-type yPGK obtained at various Gdn-HCl concentrations, monitored by variation of ellipticity at 220 nm (**A**) and by the shift in maximum fluorescence emission wavelength (**B**).

leads to a protein state that displays a fluorescence signal corresponding to fully exposed tryptophans, whereas under the same denaturant concentrations, the CD signal is only partially lost.

Time-Resolved Fluorescence

To describe more precisely the cold effect on yPGK stability, time-resolved fluorescence measurements of tryp-

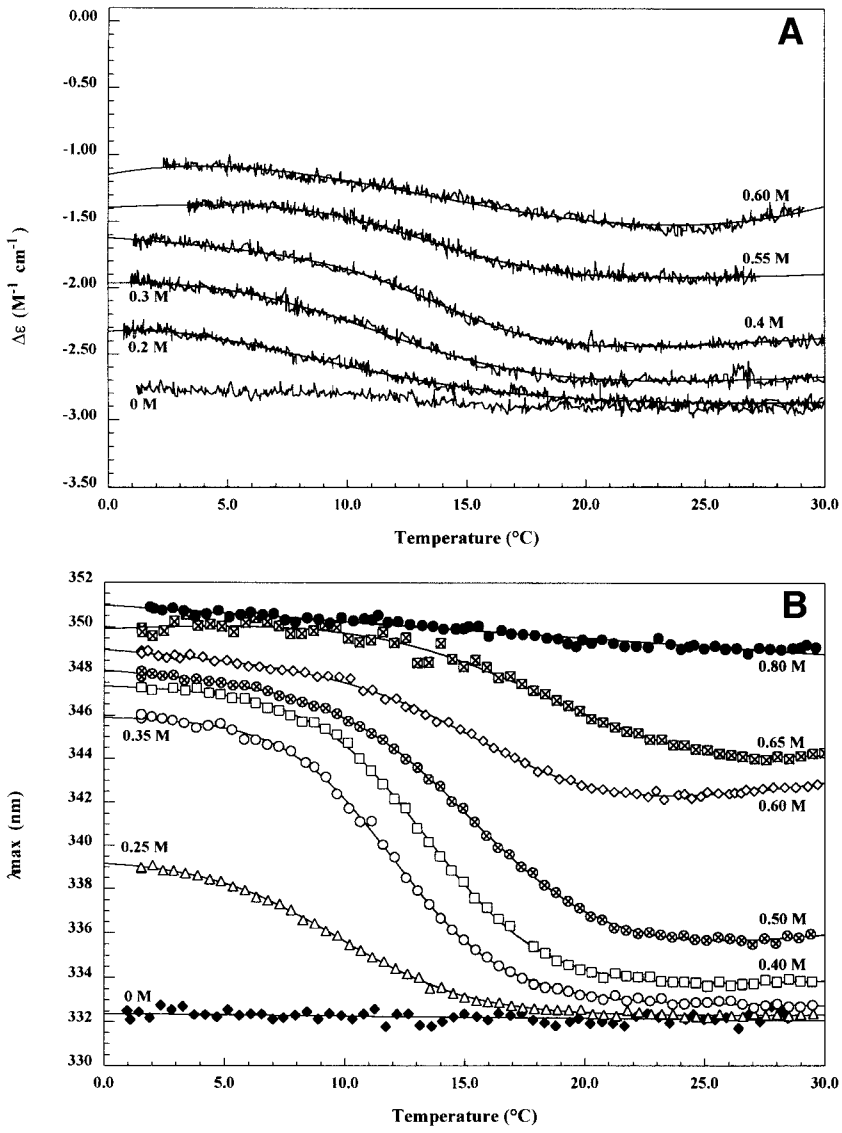

Fig. 4. Melting curves of yPGK Δ404 obtained at various Gdn-HCl concentrations, monitored by variation of ellipticity at 220 nm (**A**) and by the shift in maximum fluorescence emission wavelength (**B**).

tophans fluorescence were performed at various temperatures by using the denaturant concentrations at which the observed differences between CD and fluorescence signals are largest.

Time-resolved fluorescence decay of native wild-type yPGK can be accounted for by four lifetimes (Table II). The two main lifetimes (τ_1 = 0.1 ns and τ_{2N} = 0.47 ns), have been assigned to the two tryptophans in their native environment, whereas two lifetimes with much smaller amplitudes (τ_3 = 1.3 and τ_4 = 3.5 ns) can be associated with flexible states of the protein having different local interactions and dynamics at the level of tryptophan residues.[25] Three lifetimes with approximately equal amplitude (τ_{2D} = 0.44, τ_3 = 1.3, and τ_4= 3.5 ns) describe the fluorescence decay of the denatured protein. The ratio between these various lifetimes is dependent on temperature (Fig. 5). At 21°C and 0.45 M Gdn-HCl, tryptophan fluorescence can be resolved into four lifetimes, with a higher amplitude of the lifetimes corresponding to more flexible species. The relative amplitude of the long lifetime increases with decreasing temperature. At 4°C, the lifetime amplitude distribution is practically identical to that of the fully denatured protein.

Time-resolved fluorescence of native yPGK Δ404 can also be described by four main lifetimes (Table II), the contribution of the two long lifetimes accounting for about 10% of the total preexponential amplitude. In 0.3 M Gdn-HCl, the lifetime distribution is much deeply modified than for wild-type yPGK: the two long lifetimes account for 45% of the total fluorescence, which indicates that the protein is more flexible. Lowering temperature mainly leads to a decrease in the contribution of the shorter lifetime, suggesting that the environment of the tryptophans is altered (Fig. 5).

Small Angle X-Ray Scattering

SAXS experiments have been carried out to obtain information on the global conformation of cold-denatured

TABLE II. Tryptophan Fluorescence Decay Parameters for Wild-Type yPGK and yPGK Δ404 at Various Temperatures[†]

Parameter	Temperature (°C)	τ_1 (ns)	A_1 (%)	τ_2 (ns)	A_2 (%)	τ_3 (ns)	A_3 (%)	τ_4 (ns)	A_4 (%)
Native WT[a]	20	0.10	26.5	0.47	70.1	2.2	2.3	5.3	1
Denatured WT[a]	20	—	—	0.44	17.6	1.3	37.6	3.5	44.7
WT + 0.45 M Gdn-HCl	2.8	0.22	10.0	0.67	38.5	2.5	28.4	5.8	23
	8	0.21	14.1	0.64	41.1	2.5	25.3	5.5	19
	12	0.19	18.9	0.61	50.0	2.2	18.7	5.4	13
	16	0.19	19.7	0.56	55.4	2.5	15.7	5.4	9
	21	0.21	18.8	0.52	56.7	2.4	16.2	5.3	8
Native Δ404	20	0.14	32.2	0.53	54.6	2.2	9.0	4.7	4.2
Δ404 + 0.30 M Gdn-HCl	4.3	0.19	8.4	0.66	29.9	2.5	36.8	6.0	24.7
	8.8	0.17	12.6	0.71	33.3	2.5	33.3	5.8	20.6
	10.8	0.23	11.2	0.69	34.2	2.4	34.4	5.6	20.1
	13.4	0.29	13.5	0.70	33.3	2.4	33.6	5.4	19.6
	19.9	0.34	15.7	0.72	35.0	2.4	34.2	5.4	14.9

[†] Data are from Garcia et al., 1998.[25] WT, wild type.

yPGK. The measurements were performed at 20°C and 4°C with specific denaturant concentrations for each protein according to the circular dichroism and fluorescence results previously shown. We also performed measurements on native wild-type yPGK and yPGK Δ404 and on wild-type yPGK fully denatured at 20°C.

The absence of protein association in the samples corresponding to wild-type yPGK was checked by monitoring the scattered intensity at zero angle I(0) during data collection. No significant aggregation was detected in the samples during the course of the experiments. The value of the radius of gyration of native wild-type yPGK derived from the slope of $\ln I(q)$ versus q^2 is 24.8 ± 0.3 Å, identical to previously published values.[16]

To preserve a good signal/noise ratio, SAXS measurements cannot be performed at high Gdn-HCl concentrations because of Cl^- absorption. According to CD and fluorescence signals, yPGK at a denaturant concentration of 2 M is completely unfolded. Under this condition, yPGK exhibits a threefold increase of the radius of gyration (Rg = 71.0 ± 1 Å), in agreement with a previous study of fully denatured yPGK by using small angle neutron scattering[31] in the presence of 4 M Gdn-HCl.

In the presence of 0.45 M Gdn-HCl, the scattering profile of wild-type yPGK at 20°C is identical to that of the native protein. At 4°C, this apparent Rg (25.3 ± 0.2 Å) is hardly larger than that of native yPGK. In contrast, a slight increase of the denaturant concentration to 0.6 M leads to a 50% increase of the apparent radius of gyration of wild-type at 20°C (Rg = 36.6 ± 1 Å) followed by a twofold increase on cold denaturation (63.9 ± 2Å at 4°C).

Similar measurements were performed on yPGK Δ404. In that case, scattering intensities at very low angle indicated the presence of some protein association, especially under slightly destabilizing conditions. This prevented us from performing measurements at denaturant concentrations higher than 0.2 M at 4°C. We took care, in applying the Guinier approximation, to discard data points corresponding to very low angle (q less than 0.022 $Å^{-1}$). I(0) values derived from these analyses yielded molecular weight estimates in agreement with the value calculated from the sequence.

The value of the radius of gyration of native yPGK Δ404 at 20°C is 29.1 ± 1Å, 4 Å larger than that of the wild-type protein. Furthermore, the scattering profile exhibits clear differences with that of wild-type yPGK. At 20°C and up to 0.30 M Gdn-HCl, the Rg value remains constant within error bars. In 0.4 M Gdn-HCl, a significant increase of the apparent Rg to 31.7 ± 0.6Å is observed. At 4°C, and in the absence of denaturant, the Rg value is equal to 31.8 ± 0.6Å. This value increases to 34.1 ± 0.5 Å in 0.2 M Gdn-HCl.

Kratky plot analysis of SAXS data can provide information on the shape of the polypeptide chain: when plotting $q^2I(q)$ *versus* q the scattering profile of a globular protein exhibits a characteristic bell shape at high q-values, whereas it displays a plateau for an expanded chain.[35] Kratky plots of wild-type yPGK and yPGK Δ404 are shown on Figure 6. At 20°C, and up to 0.6 M Gdn-HCl, the profile of wild-type yPGK corresponds to a globular protein population. At 4°C and in the presence of 0.45 M Gdn-HCl, the Kratky plot is superimposable on the native wild-type profile. In contrast, in the presence of 0.6 M Gdn-HCl, the plateau indicates a lack of globularity of the protein. Kratky plots for yPGK Δ404 show that there is always a high proportion of globular protein in solution even at 4°C in the presence of 0.2 M Gdn-HCl, as the scattering profile exhibits a clear maximum.

DISCUSSION

Low-Temperature Effect on Wild-Type yPGK and yPGK Δ404

It is now well known that proteins can be denatured by lowering temperature, such cold denaturation generally occurring below 0°C for proteins in pure aqueous solution.[2] However, the cold effect on protein stability can be observed at temperatures above 0°C by performing Gdn-HCl denaturation at various temperatures. For example, transition curves obtained by monitoring the variation in ellipticity (Fig. 1A) show that wild-type yPGK is destabilized by lowering the temperature from 20°C to 4°C, with a ΔG_0 value decreasing by about 3 kcal/mol. Such destabilization is mainly reflected by a shift in the Cm value of the

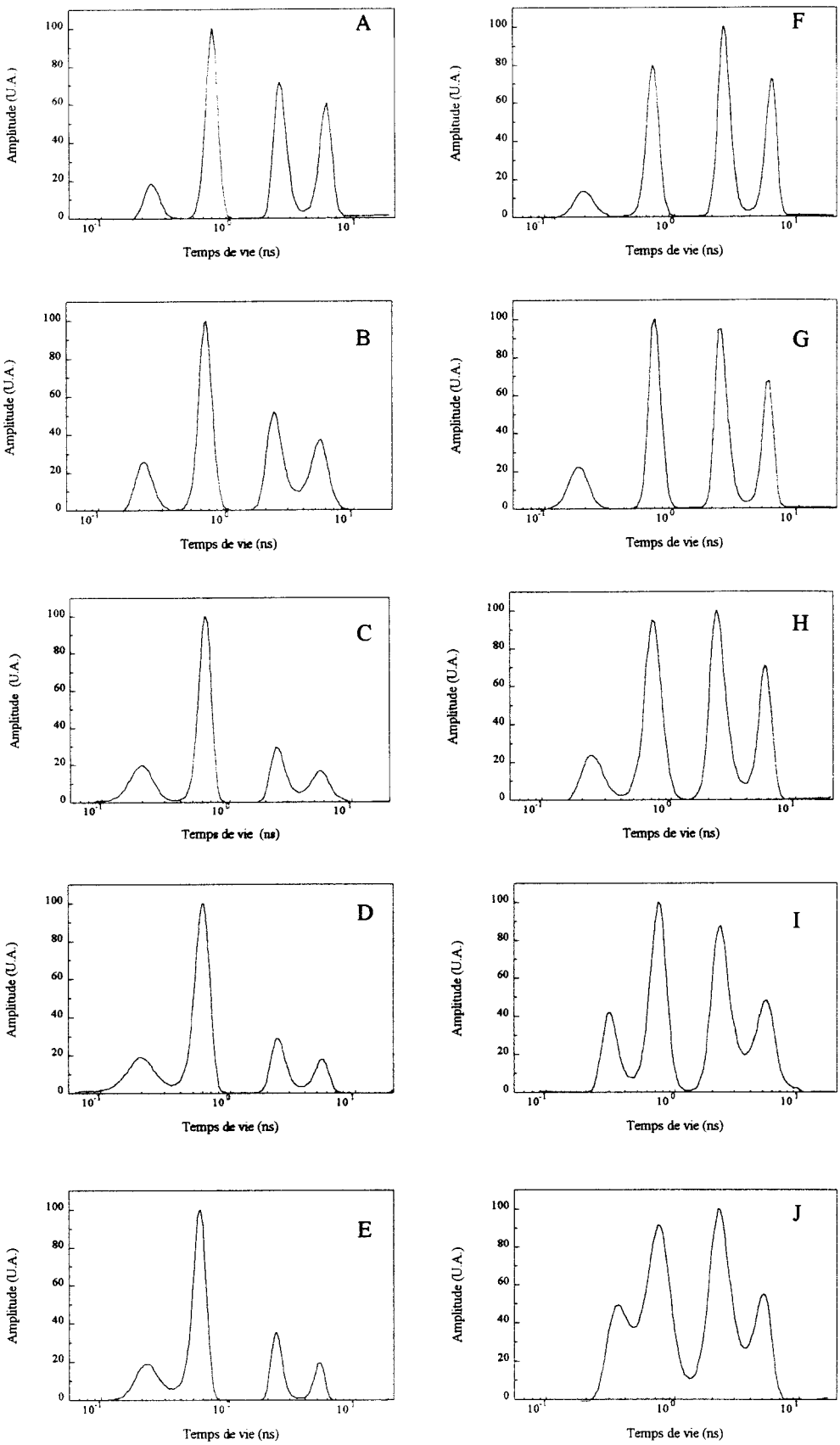

Fig. 5. Tryptophan fluorescence lifetime distribution of wild-type yPGK in 0.45 M Gdn-HCl (A–E) and yPGK Δ404 in 0.3 M Gdn-HCl (F–J) at various temperatures: 4°C (**A,F**), 8°C (**B,G**), 12°C (**C,H**), 16°C (**D, I**), and 21°C (**E,J**).

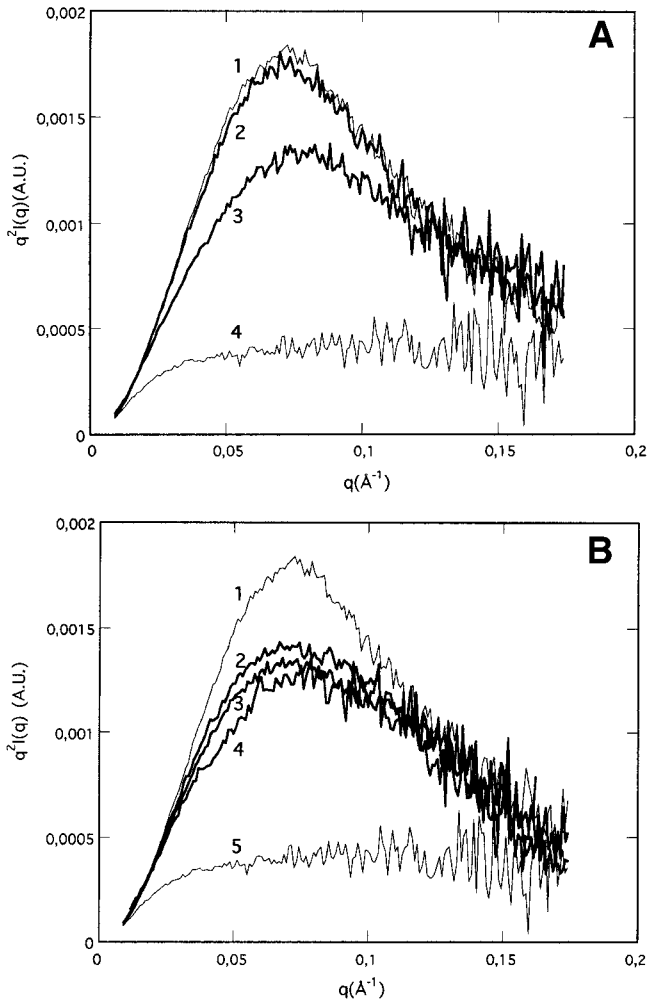

Fig. 6. **A:** Kratky plot $q^2I(q)$ *versus* q of wild-type (WT) yPGK in the native state (1), in 0.6 M Gdn-HCl at 20°C (2), in 0.6 M Gdn-HCl at 4°C (3), and in the fully denatured state (4). **B:** Kratky plot $q^2I(q)$ versus q of yPGK Δ404 in the native state at 20°C (2), at 4°C without Gdn-HCl, and in 0.2 M Gdn-HCl at 4°C (4). The curves of WT yPGK in the native state (1) and in the fully denatured state (5) are also given for comparison. Each curve was normalized by the $I_{(0)}$ value obtained from the Guinier or Debye analysis.

transition curve without significant change in the m value (Table I).

Regarding fluorescence data, the transition curves induced by Gdn-HCl are asymmetric at both temperatures, the second transition being related to residual structures. The first transition, with a Cm of 0.6 M, corresponding to a global destabilization of the protein structure, is cold sensitive. In contrast, the second transition occurring around 1.1 M Gdn-HCl is not affected by low temperature. This step is associated with the destruction of residual structures stabilized by electrostatic interactions around buried tryptophans.[11]

The C-terminal deleted mutant yPGK Δ404 appears to be more cold-sensitive than wild-type yPGK, quantitative and qualitative changes being observed in the overall denaturation process. As for wild-type yPGK, lowering the temperature from 20 to 4°C leads to a shift in the Cm value of the transition monitored by ellipticity. However, in the case of yPGK Δ404, this shift is accompanied by a large decrease in the cooperativity of the transition, as indicated by the decrease of the m values (from 5 to 3 kcal/mol/M). Above 1.5 M Gdn-HCl, the ellipticity value is the same at both temperatures, suggesting that the protein reaches the same denatured state. In this case, the decrease in m value indicates that at 4°C, yPGK Δ404 has an overall accessible surface to solvent higher than at 20°C. This finding is consistent with the increase in Rg value from 29.1 Å to 31.8 Å when lowering the temperature from 20°C down to 4°C.

Cold Denaturation of Wild-Type yPGK and yPGK Δ404

The results displayed in Figures 1 and 2 suggest that cold denaturation of both wild-type yPGK and yPGK Δ404 can be observed in the presence of low denaturant concentrations. Thus, cold denaturation was directly followed in the presence of various denaturant concentrations. For wild-type yPGK, by monitoring the shift in the maximum of fluorescence emission, symmetrical transitions curves were obtained (Fig. 3B). However, when the transition was monitored by variation in ellipticity at 220 nm, the resulting curves were asymmetrical (Fig. 3A). Such asymmetry suggests that intermediate states are involved in the cold denaturation process. Wild-type yPGK contains 2 tryptophans, both located in the C-terminal domain; thus, the fluorescence signal is mainly related to events occurring in this domain. In contrast, the ellipticity signal reflects the secondary structure content of the whole protein. Melting curves show that, for a given denaturant concentration, changes around tryptophans (Fig. 3B) occur at a higher temperature than changes in ellipticity (Fig. 3A). This finding is consistent with previously published studies suggesting that the C-terminal domain is more cold-sensitive than the N-terminal domain.[19]

Further information about the cold denaturation process can be obtained by using various Gdn-HCl concentrations. In particular, for denaturant concentrations lower that 0.6 M, the denaturation is not complete. More specifically, the comparison between CD and fluorescence shows that it is possible to stabilize a species for which the fluorescence signal corresponds mainly to exposed tryptophans, whereas the CD signal, reflecting overall secondary structure, is only partially modified. Because the tryptophan residues are located in the C-terminal domain, this suggests that the stabilized species possesses a C-terminal domain with a strongly perturbed structure, whereas its N-terminal domain essentially retains its native conformation. This uncoupling between domains is even more significant in yPGK Δ404. In the presence of 0.3 M Gdn-HCl, cold denaturation leads to a species displaying about 50% of native ellipticity, whereas the fluorescence signal corresponds to that of a nearly fully denatured protein (Fig. 4).

Role of Interdomain Hydrophobic Interactions

It is well known that cold affects mainly hydrophobic interactions; data obtained on both proteins seem to

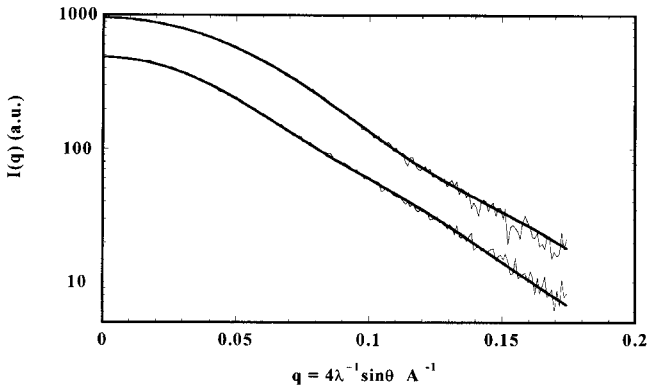

Fig. 7. Calculated (thick lines) and experimental (thin lines) scattering patterns of wild-type yPGK (top curves) and yPGK Δ404 recorded at 20°C in 20 mM Tris-HCl buffer, pH 7.5, containing 0.5 mM ethylenediaminetetraacetic acid and 1 mM dithiothreitol (see text for details). The two pairs of curves have been shifted vertically for the sake of clarity.

indicate that hydrophobic interactions are more important for the stabilization of the C-terminal domain than for the N-terminal domain. However, this sensitivity to low temperature is stronger in yPGK Δ404. Previous studies have shown that yPGK Δ404 behaves as two isolated domains[13,20] with an overall higher flexibility than wild-type yPGK. Time-resolved fluorescence measurements support this view. The distribution of fluorescence lifetimes of native yPGK Δ404 contains a high proportion of long lifetimes (Fig 5.) Although it was proposed earlier that these lifetimes are related to denatured states,[36] they have been shown recently to be associated with flexible states of the protein where tryptophan residues have different environment and dynamics.[25] Taking these results into account, the difference between the fluorescence lifetime distributions of wild-type yPGK and yPGK Δ404 can be attributed to changes in protein flexibility induced by the loss of the C-terminal helix.

This flexibility can be further characterized by SAXS. By using the program CRYSOL, the scattering pattern of the crystal structure of wild-type yPGK has been calculated and found to be identical to the experimental scattering curve within error bars as shown on Figure 7 (top curves). With regard to the mutant yPGK Δ404, after suppression of the last 12 residues, we tested the simple assumption that, as a consequence of the deletion, the two domains which are connected by a flexible linker are rotating fairly freely in solution as rigid bodies. Several open model structures were produced by rotating the C-terminal domain with respect to the N-terminal domain around the Cα of threonin 202 at the C-terminal end of the linker (see Materials and Methods section), and their scattering curve was calculated together with that of the unrotated structure. No single pattern fitted the experimental curve, but the average of the scattering pattern of the unperturbed structure and of the open structure shown in Figure 8 produced a resulting curve identical to the experimental one within error bars (Fig. 7, bottom curves). This result supports our view of a mutant protein exploring a distribution of conformations ranging from the closed, original structure to wide open ones through multiple dynamic equilibria.

For wild-type yPGK, lowering temperature to 4°C increases the proportion of the long fluorescence lifetimes. However, low temperature has a less significant effect on long fluorescence lifetimes distribution of yPGK Δ404. This indicates that cold denaturation does not lead to a significant increase in flexibility around tryptophans in this mutant.

The strong uncoupling between the domains observed in the yPGK Δ404 and the same uncoupling observed on cold denaturation of both proteins allows one to obtain information about the nature of stabilizing interaction between the domains. Analysis of the native structure reveals that the two domains interact primarily through hydrophobic and hydrogen bond interactions at the interface. However, the cold effect is mainly related to hydrophobic interactions. Thus, these data suggest that these interactions play an important role in stabilizing the domains. Low temperature has qualitatively the same effect as the deletion of the last 12 residues of the protein. This finding indicates that the 404–415 sequence contains critical residues stabilizing hydrophobic interactions. A close examination of the structure around residues 404–415 reveals that residue Leu405 is in tight interaction with helix XIII and is part of an hydrophobic pocket with residues Ala 395 and Leu 399. Among other possible hydrophobic interactions are those involving Leu 411, strictly conserved among the different species and which is included within an hydrophobic pocket made of Val 408, Ala 409, Leu 187, and Ala 183.

Nature of the Cold Denatured State

More information can be obtained by performing SAXS measurements. This technique provides crucial information on the shape and compactness of macromolecules in solutions.[37,38] So far, apart from Damaschun's work on yPGK previously mentioned, only one study has established the compactness of a cold-denatured protein by SAXS: Konno and co-workers have shown that *Streptomyces* subtilisin inhibitor exists at low pH in at least three distinct thermodynamic states: native, cold denatured, and heat denatured.[39,40] They have established that cold-denatured *Streptomyces* subtilisin inhibitor is still partially structured and rather compact but becomes a disordered expanded chain when further denatured by urea. Because compactness is an important feature of denatured protein, we have used SAXS to characterize the overall dimension and global conformation of the cold-denatured states of yPGK under different destabilizing conditions. A comparison between the data obtained with the various techniques used in this study allows the description of the different protein states.

However, the protein solutions used in these different experimental approaches vary by an order of magnitude. Although the denaturation process of monomeric proteins, a monomolecular reaction, shows no concentration dependence, protein interactions are strongly concentration dependent, which could make this comparison question-

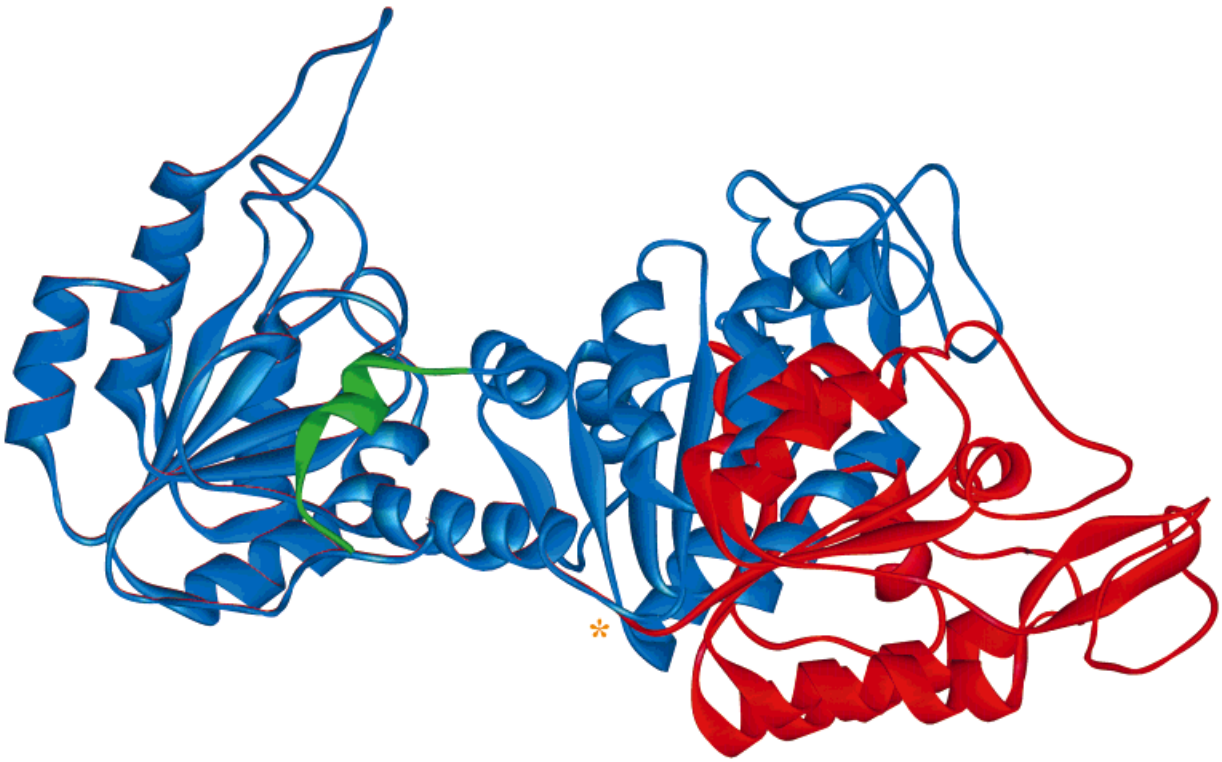

Fig. 8. Ribbon representation of wild-type and mutant conformations. Blue: wild-type yeast PGK; the last 12 residues missing from yPGK Δ404 are shown in green. The blue ribbon also represents the closed conformation of yPGK Δ404. Red: open conformation of yPGK Δ404. The orange star shows the location of Thr202-Cα around which the C-terminal domain was rotated. The figure has been made by using the SwissProtPdbViewer.[46]

able. The oligomerization state of the solution of WT PGK has been checked by monitoring the scattered intensity at zero angle I(0) during data acquisition: no aggregation was detected. Although a slight association of the mutant protein has been observed, excluding the innermost part of the scattering curve allowed a satisfactory Guinier analysis yielding I(0) values in agreement with the molecular weight of the protein (see Results section). These controls validate the following comparison between the different experimental results.

First, according to CD, static fluorescence, and SAXS data, yPGK in the presence of 0.45 M Gdn-HCl at 20°C is as structured as native yPGK. Previous studies[13] have already shown that under these conditions, yPGK is fully active. The only effect of such denaturant concentrations is a slight increase in protein flexibility as indicated by the fluorescence lifetimes. At 4°C, the CD signal indicates that the protein has lost a great part of its secondary structure, mainly α-helices, and according to steady-state fluorescence, the tryptophans are well exposed to the solvent, the protein displaying the same fluorescence lifetime distribution as the completely denatured protein. In contrast, SAXS measurements show that Rg is the same as for native yPGK. Consequently, under these experimental conditions, the protein is in equilibrium between at least three species: the native form (N), the denatured one (D), and an intermediate state X. Let us emphasize here again that the last two species must be thought of as typifying an ensemble of configurations sharing dynamic and structural characteristics, the appropriate averages of which are experimentally accessible. For example, according to data from Figure 3A and taking into account that denatured species are devoid of CD signal, the proportion of native species is at most 70% at 4°C in the presence of 0.45 M Gdn-HCl. On the assumption that the solution only contains the two N and X species, an upper limit for the Rg value of the intermediate of about 27 Å can be derived from the apparent Rg_{app}, its square value being a weighted mean of the actual Rg_i^2 values of both species (see Materials and Methods section). Accounting for the presence of some fraction of denatured species would only further reduce the value of this upper limit. Thus, although the Rg is a mean value, it can be soundly concluded that the global structure of the protein in the intermediate (ensemble of) state(s) is highly compact. This is confirmed by the Kratky-plot profiles, indicating that the protein is definitively globular under these experimental conditions. Qualitatively, the same state is obtained with yPGK Δ404, the difference between compactness in the one hand and tryptophan accessibility/flexibility in the other hand being even more marked, which might be due to the large uncoupling of the domains.

From these results, it is clear that not only is cold denaturation in yPGK not a two-state process but that the cold-denatured protein obtained in our experimental conditions corresponds to a compact denatured state. Although

compact denatured states have already been described for various proteins, even for cold denaturation, the denatured state observed for yPGK is quite unusual. For example, it has been shown that residual structures existing in the denatured state of Barstar corresponds to native secondary structures.[41] In the case of yPGK, it is quite difficult to determine precisely the exact nature of the compact state. First, ellipticity has been measured at 220 nm, a wavelength where the majority of the signal comes from α helices and where modifications in the β sheets are hardly detected. Second, the cold-denatured protein does not display a CD spectrum characteristic of a fully denatured protein. Thus, cold denaturation could mainly lead to a destabilization of the helices, located on the surface of the protein, whereas the β sheets, which are mainly buried, would be more cold resistant. With this assumption, the structure of the cold-denatured yPGK could be pictured as significantly perturbed in its periphery (fluorescence lifetimes) while preserving an essentially intact core, the whole molecule retaining a high degree of compactness (radius of gyration). Although the large difference in stability between the two domains at low temperature would suggest that these residual structures are mainly located in the N-terminal domain, the value of the radius of gyration is not compatible with a fully extended C-terminal domain. Thus, the above description is likely to hold true for the C-terminal domain as well.

Although various techniques have shown the existence of residual structures in denatured proteins, this is one of the first examples of a compact denatured state devoid of its main content in alpha helices. Because it is generally accepted that residual structures are related to the initial events that occur during folding,[42] this state could correspond to the initial collapse of the molecule. A more precise description of this compact denatured state could be reached by using a singular value decomposition analysis[43–45] of a full set of SAXS patterns recorded as a function of temperature. Thus, the exact nature of the interactions existing in this intermediate and its internal dynamics require further work, which is under way in our laboratory.

ACKNOWLEDGMENTS

We thank Dr. Fabienne Merola for the help provided for measuring and analyzing time-resolved fluorescence data and Dr. Charles Robert for carefully reading the manuscript.

REFERENCES

1. Privalov PL. Cold denaturation of proteins. Crit Rev Biochem Mol Biol 1990;25:281–305.
2. Franks F. Protein destabilization at low temperatures. Adv Protein Chem 1995;46:105–139.
3. Brandts JF. The thermodynamics of protein denaturation. J Am Chem Soc 1964;86:4291–4301.
4. Privalov PL. Stability of proteins. Adv Prot Chem 1979;33:167–241.
5. Privalov PL, Griko YV, Venyaminov SY. Cold denaturation of myoglobin. J Mol Biol 1986;190:487–498.
6. Bonnete F, Madern D, Zaccai J. Stability against denaturation mechanisms in halophilic malate dehydrogenase "adapt" to solvent conditions. J Mol Biol 1994;244:436–447.
7. Huang GS, Oas TG. Heat and cold denatured states of monomeric λ repressor are thermodynamically and conformationally equivalent. Biochemistry 1996;35:6173–6180.
8. Griko YV, Kutyshenko VP. Differences in the process of β-lactoglobulin cold and heat denaturation. Biophys J 1994;67:356–363.
9. Tamura A, Kimura K, Takahara H, Akasaka K. Cold denaturation and heat denaturation of *Streptomyces* subtilisin inhibitor. Biochemistry 1991;30:11307–11313.
10. Tamura A, Kimura K, Takahara H, Akasaka K. Cold denaturation and heat denaturation of *Streptomyces* subtilisin inhibitor. Biochemistry 1991;30:11313–11320.
11. Garcia P, Desmadril M, Minard P, Yon JM. Evidence for residual structures in an unfolded form of yeast phosphoglycerate kinase. Biochemistry 1995;34:397–404.
12. Pecorari P, Minard P, Desmadril M, Yon JM. Occurrence of transient multimeric species during the refolding of a monomeric protein. J Biol Chem 1995;271:5270–5276.
13. Ritco-Vonsovici M, Mouratou B, Minard P, Desmadril M, Yon JM, Andrieux M, Leroy E, Guittet E. Role of the C-terminal helix in the folding and stability of yeast phosphoglycerate kinase. Biochemistry 1995;34:833–841.
14. Griko YV, Venyaminov SU, Privalov PL. Heat and cold denaturation of phosphoglycerate kinase. FEBS Lett 1989;244:276–278.
15. Freire E, Murphy KP, Sanchez-Ruis JM, Galisteo ML, Privalov PLL. The molecular basis of cooperativity in protein folding. Dissection of interdomain interactions in phosphoglycerate kinase. Biochemistry 1992;31:250–256.
16. Damaschun G, Damaschun H, Gast K, Misselwitz R, Muller JJ, Pfeil W, Zirwer D. Cold denaturation-induced conformational changes in phosphoglycerate kinase from yeast. Biochemistry 1992;32:7739–7746.
17. Damaschun G, Damaschun H, Gast K, Zirwer D. Denatured states of yeast phosphoglycerate kinase. Biochemistry (Engl Transl Biokhimiya) 1998;63:259–275.
18. Gast K, Damaschun G, Damaschun H, Misselwitz R, Zirwer D. Cold denaturation on yeast phosphoglycerate kinase: kinetics of changes in secondary structure and compactness on unfolding and refolding. Biochemistry 1993;32:7747–7752.
19. Gast K, Damaschun G, Desmadril M, Minard P, Müller-Frohne M, Pfeil W, Ziwer D. Cold denaturation of yeast phosphoglycerate kinase. FEBS Lett 1995;358:247–250.
20. Andrieux M, Leroy E, Guittet E, Ritco-Vonsovici M, Mouratou B, Minard P, Desmadril M, Yon JM. Transferred nuclear Overhauser effect study of the C-terminal helix of yeast phosphoglycerate kinase: NMR solution structure of the C-terminal bound peptide. Biochemistry 1995;34:842–846.
21. Nozaki Y. The preparation of guanidine hydrochloride. Methods Enzymol 1970;26:43–50.
22. Pace CN. Determination and analysis of urea and guanidine hydrochloride denaturation curves. Methods Enzymol 1986;131:266–280.
23. Press WH, Flannery BP, Teulosky SK, Veterling WT. Numerical recipes. Cambridge: Cambridge University Press; 1986.
24. O'Connor DV, Phillips D. Time-correlated single photon counting. London: Academic Press; 1984.
25. Garcia P, Merola F, Receveur V, Blandin P, Minard P, Desmadril M. Steady-state and time-resolved fluorescence study of residual structures in an unfolded form of yeast phosphoglycerate kinase. Biochemistry 1998;37:7444–7455.
26. Depautex C, Desvignes C, Leboucher P, Lemonnier M, Dagneaux D, Benoit JP, Vachette P. The small angle X-ray scattering instrument D24. Annual report p75 Laboratoire pour l'Utilisation du Rayonnement Electromagnetique, Orsay, France; 1987.
27. Boulin CR, Kempf MH, Koch J, McLaughlin SM. Data appraisal, evaluation and display for synchrotron radiation experiments: hardware and software. Nucl Instr Meth A1986;249:399–407.
28. Dubuisson JM, Decamps T, Vachette P. Improved signal-to-background ratio in small angle X-ray scattering experiments with synchrotron radiation using an evacuated cell for solutions. J Appl Crystallogr 1997;30:49–54.
29. Guinier A, Fournet G. Small angle scattering of X-rays. New York: Wiley Interscience; 1955.
30. Debye P. Light scattering in solution. J Applied Physiol 1944;15:338–342.
31. Receveur V, Durand D, Desmadril M, Calmettes P. Repulsive

interparticle interactions in a denatured protein solution revealed by small angle neutron scattering. FEBS Lett 1998;426:57–61.
32. Svergun DI, Barberato C, Koch MHJ. CRYSOL: a program to evaluate X-ray solution scattering of biological macromolecules from atomic coordinates. J Appl Crystallogr 1995;28:768–773.
33. Watson HC, Walker NPC, Shaw PJ, Bryant TN, Wendell PL, Fothergill LA, Perkins RE, Conroy SC, Dobson MJ, Tuite MF, Kingsman AJ, Kingsman SM. Sequence and structure of yeast phosphoglycerate kinase. EMBO J 1982;1:1635–1640.
34. Roussel A, Fontecilla-Camps JC, Cambillau C. CRYStallize: a crystallographic symmetry display and handling subpackage in TOM/FRODO. J Mol Graph 1990;8:86–88.
35. Kataoka M, Goto Y. X-ray solution scattering studies of protein folding. Fold Des 1996;1:107–114.
36. Szpikowska BK, Beechem JM, Sherman MA, Mas MT. Equilibrium unfolding of yeast phosphoglycerate kinase and its mutant lacking one or both native tryptophans: a circular dichroism and steady-state and time resolved fluorescence study. Biochemistry 1994;33:2217–2225.
37. Koide S, Bu Z, Risal D, Pham TN, Nakagawa T, Tamura A, Engelman DM. Multistep denaturation of Borrelia burgdorferi OspA, a protein containing a single-layer beta-sheet. Biochemistry 1999;38:4757–4767.
38. Kamatari YO, Ohji S, Konno T, Seki Y, Soda K, Kataoka M, Akasaka K. The compact and expanded denatured conformations of apomyoglobin in the methano-water solvent. Protein Sci 1999;8:873–882.
39. Konno T, Kamatari YO, Kataoka M, Akasaka K. Urea-induced conformational changes in cold- and heat-denatured states of a protein, *Streptomyces* subtilisin inhibitor. Protein Sci 1997;6:2242–2249.
40. Konno T, Kataoka M, Kamatari Y, Kanaori K, Nosaka A, Akasaka K. Solution X-ray scattering analysis of cold- heat-, and urea-denatured states in a protein, *Streptomyces* subtilisin inhibitor. J Mol Biol 1995;251:95–103.
41. Wong KB, Freund SMV, Fersht AR. Cold denaturation of Barstar: 1H, 15N, 13C NMR assignment and characterization of residual strictures. J Mol Biol 1996;259:805–818.
42. Arcus VL, Vuilleumier S, Freund SM, Bycroft M, Fersht AR. A comparison of the pH, urea, and temperature-denatured states of barnase by heteronuclear NMR: implications for the initiation of protein folding. J Mol Biol 1995;254:305–321.
43. Fetler L, Tauc P, Herve G, Moody MF, Vachette P. X-ray scattering titration of the quaternary structure transition of aspartate transcarbamylase with a bisubstrate analogue. Influence of nucleotide effectors. J Mol Biol 1995;251:243–255.
44. Fowler AG, Foote AM, Moody MF, Vachette P, Provencher SW, Gabriel A, Bordas J, Koch MHJ. Stopped-flow solution scattering using synchrotron radiation: apparatus, data collection and data analysis. J Biochem Biophys Methods 1983;7:317–329 and its Appendix, Provencher SW, Glöckner J. Analysis of the components present in kinetics (or titration) curves, analysis. J Biochem Biophys Methods 1983;7:331–334.
45. Segel DN, Fink AL, Hodgson KO, Doniach S. Protein denaturation: a small-angle X-ray scattering study of the ensemble of unfolded states of cytochrome c. Biochemistry 1998;37:12443–12451.
46. Guex N, Peitsch MC. SWISS-MODEL and the Swiss-PdbViewer: an environment for comparative protein modelling. Electrophoresis 1997;18:2714–2723.